35th Annual International Conference of the IEEE EMBS
Osaka, Japan, 3 - 7 July, 2013

Retinal vessel classification: sorting arteries and veins*

D. Relan, T. MacGillivray, L. Ballerini and E. Trucco

Abstract—**For the discovery of biomarkers in the retinal vasculature it is essential to classify vessels into arteries and veins. We automatically classify retinal vessels as arteries or veins based on colour features using a Gaussian Mixture Model, an Expectation-Maximization (GMM-EM) unsupervised classifier, and a quadrant-pairwise approach. Classification is performed on illumination-corrected images. 406 vessels from 35 images were processed resulting in 92% correct classification (when unlabelled vessels are not taken into account) as compared to 87.6%, 90.08%, and 88.28% reported in [12] [14] and [15]. The classifier results were compared against two trained human graders to establish performance parameters to validate the success of classification method. The proposed system results in specificity of (0.8978, 0.9591) and precision (positive predicted value) of (0.9045, 0.9408) as compared to specificity of (0.8920, 0.7918) and precision of (0.8802 , 0.8118) for (arteries, veins) respectively as reported in [13]. The classification accuracy was found to be 0.8719 and 0.8547 for veins and arteries, respectively.**

I. Introduction

Many important eye diseases as well as systemic diseases manifest themselves in the retina [1]. Developments in image processing and automated diagnostic systems offer great potential for retinal fundus imaging to be used in large-scale screening programmes, with significant resource savings and freedom from observer bias [2]. A number of automatic retinal image analysis algorithms have been proposed for extracting the vascular structure and measuring different morphological parameters [3-6]. Crucially, the vasculature change that appears during the onset of a systemic disease can affect arteries and veins differently. For example, one of the early signs of retinopathy is generalized arteriolar narrowing in which the arteriolar to venular width (AVR) decreases. There is also mounting evidence that narrowed retinal arterioles are associated with long-term risk of hypertension, while AVR is a well-established predictor of stroke and other cardiovascular events [4] [7-8]. An essential part of automatic systems for vasculature characterization is therefore a computational method for classifying vessels into arteries and veins.

Previous work has reported on supervised vessel classification [9-11], but such algorithms require large volumes of clinical annotations on images (i.e. manual classification of vessels into veins and arteries) to generate suitable training data and this may not be easy to source. Thus, we propose an algorithm for unsupervised artery-vein ($a|v$) classification. We extract vessel centreline pixels (by tracking the vessels between manually marked start and end points) and then classify them into arteries and veins in an unsupervised manner, i.e. without the need of training data.

In an automatic unsupervised method proposed in 2003, Grisan and Ruggeri [12] performed quadrant-wise vessel classification in a concentric zone around the optic disc using fuzzy C-Mean clustering on 443 vessels from 35 images and reported 87.6% correct classification. In another study [13] classification was performed between two concentric circumferences around the optic disc and quadrants were rotated in steps of 20° to include at least one artery and one vein in each quadrant, and the classification was performed by K-Means clustering on 58 images and positive and negative likelihood ratios, which confirm the validity of their system, were (7.2386, 4.2218) and (0.2445, 0.1528) for (arteries, veins) respectively. They also reported 87% and 90.08% correct classification before and after applying their proposed tracking method in [14]. The quadrant-wise classification imposes a condition to have at least one artery and one vein per quadrant. Also, basic K-Means clustering is sensitive to the initial centres and gets stuck easily at local optimal values. In [15], fuzzy C-Mean clustering was applied for $a|v$ classification. In order to classify vessels, the separation of vessel trees into a structurally mapped vessel network was carried out. The authors excluded centreline pixels which have similar affinity for both the clusters from the successive classification process, treating them as noisy pixels. The proposed method was applied to 15 retinal colour fundus images resulting in a classification accuracy of 88.28%.

We use the Gaussian Mixture Model - Expectation Maximization (GMM-EM) clustering method which, unlike K-means, does not rely heavily on initialization. The commonly used approach for determining the parameters (Mean, Covariance, mixture coefficient) of a Gaussian Mixture Model from a given dataset is to use the maximum-likelihood estimation. The EM algorithm is a general, iterative technique for computing maximum-likelihood. In GMM-EM classifier algorithm, a uniform distribution to the mixture is added to pick up background noise or data points which were not associated to either an artery or a vein cluster. The classifier is run for 10 different initial cluster centres and the parameters corresponding to the best fit (maximum likelihood) was chosen to compute Gaussian mixtures. The GMM-EM has previously been shown to be a successful clustering method for colour image segmentation [16]. To our best knowledge, we have used the GMM-EM method for the first time for retinal vessel classification. We restricted our analysis to Zone B, an annulus 0.5 to 1 disc

*Research work is supported by Leverhume trust grant RPG-419.

D. Relan is with the Clinical Research Imaging Centre, University of Edinburgh, U.K. (e-mail: d.relan@sms.ed.ac.uk).

T. MacGillivray is with Clinical Research Imaging Centre, University of Edinburgh, U.K. and Wellcome Trust Clinical Research Facility, University of Edinburgh, U.K. (e-mail: t.j.macgillivray@ed.ac.uk).

L. Ballerini and E. Trucco are with School of Computing, University of Dundee, U.K. (e-mail: luciaballerini@computing.dundee.ac.uk, manueltrucco@computing.dundee.ac.uk).

diameter from the optic disc margin surrounding the optic disc (henceforth OD) and we confined the classification of the vessels to this zone. This region has been used for the investigation of retinal biomarkers in several studies [4] [6] [8] and it is considered a significant region for extracting clinically relevant biomarkers from fundus images.

II. METHODOLOGY

A. Material

Thirty-five colour fundus images with resolution of 2048×3072 pixels and captured with Canon CR-DGi non-mydriatic retinal camera with 45° field of view were analysed in this study. The images were selected at random from a large database of non-mydriatic fundus images which were obtained from the Orkney Complex Disease Study (ORCADES). ORCADES is a genetic epidemiology study based on an isolated population in the north of Scotland. It aims to discover the genes and their variants which influence the risk of common, complex diseases.

All images were labelled by two trained observers (authors DR and TM) to generate a ground truth to compare the classification results. Observer 1 (DR) is a doctoral student (less experienced, ~1year), and observer 2 (TM) is an imaging scientist (more experienced, >10years) and both are involved in retinal imaging and analysis for clinical research. Both work in close collaboration with clinicians and were individually trained by experienced clinical colleagues in the identification of the retinal vessel type.

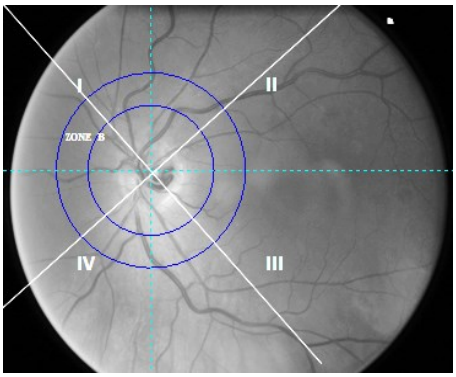

(a)

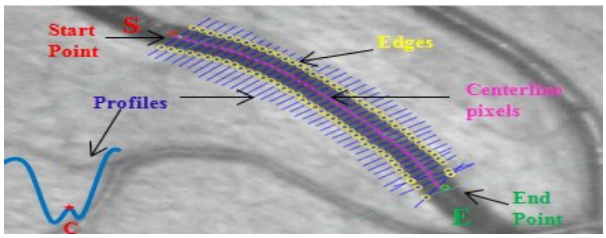

(b)

Figure 1. **(a)** Rotated quadrant by 45° (marked as white line in the image) and measurement zone: Zone B ((0.5 to 1 disc diameter from the optic disc margin surrounding the OD), **(b)** Centreline pixel extraction

B. Image pre-processing and extracting centerline pixels

The presence of inter- and intra-image contrast, luminosity and colour variability affect classification results. Thus we first compensated for background illumination based on median filtering (section 3.1 of [17]). Hue channel was processed to improve the contrast of vessels against background before illumination correction. The illumination-corrected channel was then processed to extract colour intensity features from vessels centrelines pixels.

In order to extract centreline pixels from Zone B (region between the blue concentric circles in Fig. 1(a)), each vessel was tracked between two manually marked points, start '*S*' and end '*E'* (Fig. 1(b)). To do this, first, the vector defining the direction from *S* to *E* ($V_{S\text{-}E}$) was computed as $V_{S\text{-}E} = [V_x\ V_y]$, where: $V_x = d_e\cos(\theta)$ and $V_y = d_e\sin(\theta)$, with d_e as the Euclidean distance between *S* and *E* and $\theta = \tan^{-1}(dy/dx)$, and *dx* and *dy* are differences between x and y coordinates of points *E* and *S*. Then coordinates of the new point, P_{new}, 5 pixel ahead of *S* was calculated as:

$$P_{new} = S + 5(V_{S\text{-}E}) \qquad (1)$$

At P_{new}, the intensity profile across the vessel axis (resembles an inverted Gaussian) was obtained (Fig. 1(b) shows an example). Point C, marked red on the intensity profile, was then found by locating the 2 local minima and averaging these points in order to give the approximate centre of the vessel. Then, the next P_{new} was calculated (from equation (1)) five pixels ahead of point *C* with vector direction $V_{C\text{-}E}$. This procedure continues until end point *E* was reached, i.e. cross-sectional intensity profiles were found at every 5th pixel between *S* and *E* (blue lines in Fig. 1(b)). Next, the Canny edge detector [18] was applied to each of these profiles to locate vessel edges (marked as yellow in Fig. 1(b)) and finally the centreline pixels (marked as pink in Fig. 1(b)) were located as the midpoint of a pair of edge points. In this way, the centreline pixels were extracted from vessels in each quadrant and this provided a set of *n* vessel segments: $S = V_1, V_2, \ldots, V_n$, where V_i is *i*th vessel and each vessel is represented by a set of *m* centreline pixels: $V_i = p_1, p_2, \ldots, p_m$. For each centreline pixel p_k, we store the *x* and *y* coordinates and the vessel diameter *d*.

C. Quadrant pairing and feature extraction

The image was divided into four quadrants by locating the OD and its approximate diameter [19]. Once the centreline pixels were found in each quadrant, four colour features (mean of red (*MR*), mean of green (*MG*), mean of hue (*MH*) and variance of red (*VR*)) were extracted from the corrected channels and from a circular neighbourhood around each centreline pixel, with diameter 60% of the mean vessel diameter. After feature extraction, we have four sets of feature vectors F_q , $q=1,\ldots,4$, for each pair of quadrant (i.e. for pairs (*I, II*), (*II, III*), (*III, IV*) and (*IV, I*), see Fig. 1(a)). Each sets is represented by a $4 \times N_i$ matrix, where N_i is the number of pixels in a pair of quadrants with *MG*, *MR*, *VR* and *MH* as four features, i.e. $F_q = [MG\ MR\ VR\ MH]$. Finally, each set of colour features (F_q) of pixels (representing sample points describing the vessels from pairs of quadrant) were classified using GMM-EM classifier. The classification

was performed by working separately on two quadrants at a time in a clockwise direction, i.e. classification of vessels from quadrant combinations (*I, II*), (*II, III*), (*III, IV*) and (*IV, I*). See Fig. 1(a).

GM-EMM classifies the pixels into 3 clusters: *artery*, *vein,* and *not labelled*. The centroid of arteries and veins cluster is associated with a vector of four mean values representing the four colour features. The two average values of green channel intensity representing the centroids (i.e. for two clusters) were compared to determine the *a|v* class. The cluster with higher mean green channel intensity at its centroid is defined as arterial cluster and the other as venous cluster [15]. The 3rd cluster is 'not *labelled'*.

Considering vessel pixels from a pair of quadrants for classification, one label is assigned to each pixel. As each quadrant was considered twice in the processing i.e. for pairs (*I, II*), (*II, III*), (*III, IV*) and (*IV, I*), each pixel has two labels assigned to it in total. Then the quadrant was rotated 45° clockwise (white solid lines in Fig. 1(a)) and the pixels belonging to each of the rotated quadrants were classified again, generating two more labels to each pixel. In this way each pixel has four labels from a group of: *artery (a)*, *vein (v)* and *not labelled (n)*. The quadrants are rotated so that each vessel is labelled several times which improves the chances of correct classification.

TABLE I. ASSIGNING FINAL LABEL TO A VESSEL

Pixels belonging to a vessel (I)	Four labels per pixel (II)				Final label to each pixel (artery) (III)
1.	*a*	*a*	*a*	*a*	A
2.	*a*	*a*	*v*	*a*	A
3.	*a*	*a*	*v*	*a*	A
4.	*a*	*a*	*a*	*a*	A
5.	*a*	*v*	*v*	*a*	N
6.	*a*	*n*	*n*	*a*	N
7.	*a*	*n*	*a*	*a*	A

The vessels were assigned a status of an *artery*, *vein* or *not labelled* based on the maximum number of labels of each kind to pixels belonging to a vessel. In Table I, the first column shows the pixels belonging to a vessel while the second column shows the four labels assigned to each pixel. The final label of each pixel was then decided based on following logic (column III in Table I):

1. IF number of *a* > number of *v:* then assign as *artery* (*A*). (e.g. *n v a a* = *A*)
2. IF number of *v* > number of *a:* then assign *vein* (*V*). (e.g. *n a v v* = *V*)
3. IF (number of *a* = number of *v*) (e.g. *a a v v*)
   OR IF (number of *n* > number of *a or v*)
   (e.g. (*n n n a*) or (*n n n v*))
   OR IF (number of *n* = number of *a or v*)
   (e.g. (*n n a a*) or (*n n v v*)):
   then assign *not labelled* (N)

After each pixel has been assigned a final label (*A, V* or *N*) (column III), the maximum number of labels of each kind assigned to a particular vessels was then used to decide the vessel status. Table I shows an example of vessel assignment to *artery* based upon labels (maximum number of '*A*' label) in column III.

III. RESULTS

A. Criteria for evaluating classification performance

To assess the validity of the proposed classification system following performance parameters was evaluated separately for arteries and veins (where *TP* (*True Positive*), *FP* (*False Positive*), *TN* (*True Negative*) *and FN* (*False Negative*) was calculated in a similar way as in [13]) :

$Sensitivity = TP_{a|v} / (TP_{a|v} + FN_{a|v})$,
$Specificity = TN_{a|v} / (TN_{a|v} + FP_{a|v})$,
$Positive\ Predicted\ value = TP_{a|v} / (TP_{a|v} + FP_{a|v})$,
$Negative\ Predicted\ value = TN_{a|v} / (TN_{a|v} + FN_{a|v})$,
Positive Likelihood Ratio=Sensitivity/ (1-specificity),
Negative Likelihood Ratio= (1-Sensitivity)/specificity,
$Classification\ Accuracy = (TP_{a|v} + TN_{a|v}) / (TP_{a|v} + TN_{a|v} + FP_{a|v} + FN_{a|v})$.
$Classification\ Error\ rate = (FP_{a|v} + FN_{a|v}) / (TP_{a|v} + TN_{a|v} + FP_{a|v} + FN_{a|v})$.

B. Experimental results

We used a total of 406 vessels from 35 colour fundus images to test classification. The system did not assign a final label (*artery* or *vein*) to 55 vessels, i.e. 13.5% were classified *not labeled*. 92% of the remaining 351 vessels (which were assigned a label of *artery* or *vein*) were classified correctly.

TABLE II. CLASSIFICATION PERFORMANCE PARAMETERS

Performance Measure	Arteries	Veins
Sensitivity	0.8181	0.7688
Specificity	0.8978	0.9590
Positive Predicted value	0.9045	0.9408
Negative Predicted value	0.8067	0.8307
Positive Likelihood Ratio	8.0095	18.7933
Negative Likelihood Ratio	0.2025	0.2410
Classification Accuracy	0.8547	0.8719
Classification Error rate	0.1453	0.1281

The manual labeling of vessels by two trained human observers was considered as ground truth. Observer 1 classified all vessels while 1.48% of vessels were not classified by observer 2. The performance measures (explained in Section A above) were computed separately for arteries and veins w.r.t observers' labels. For all images and w.r.t. observer 1, the performance measures are given in Table II. The sensitivity was 0.8181 for arteries, and 0.7688 for veins. That is to say, the probability of an incorrect classification was 18.2% for arteries, and 23.1% for veins. The *precision* (*positive predicted value*) for both *arteries* and *veins* from our methods (see Table II) was higher than 0.8802 and 0.8118 for *arteries* and *veins* respectively which was reported in [13]. Likelihood ratios (see Table II) were also high and confirmed the high reliability of our system. Results were slightly higher as compared with observer 2.

Our approach led to 92% correct classification which is higher as compared to 87.6%, 90.08%, and 88.28% reported in [12] [14] and [15], respectively.

IV. Discussion and Conclusion

Labelling large numbers of vessels manually is a time-consuming task. It is therefore important to include (semi-) automated classification framework with high sensitivity and specificity in system meant for (semi-) automatic analysis of large image data sets, like VAMPIRE [20][21]. We have proposed an unsupervised method using colour features to classify arteries and veins. Our system does not require the presence of at least one artery and one vein per quadrant, and is applicable even if there is no vessel in a quadrant.

In our tests, classification results were compared to manual labels and our system shows a low false positive rate, i.e. (*1-specificity*) of 0.041 and 0.102 compared to 0.208 and 0.108 reported in [13] for *vein* and *artery* respectively. Furthermore, likelihood ratios, which confirms the high reliability of our proposed system was also greater. Our system results in *positive likelihood ratio* of (18.793, 8.009) and *negative likelihood ratio* of (0.2410, 0.2025) as compared to *positive likelihood ratio* of (4.2218, 7.2386) and *negative likelihood ratio* of (0.1528, 0.2445) for (*veins*, *arteries*) respectively reported in [13]. Also, the percentage of correct classification by our system was higher than those reported in [12] [14] and [15], respectively. Results were slightly higher when compared with observer 2 (most experience). We analyzed 35 colour fundus images compared to 35, 58 and 15 images analysed in [12] [14] and [15], respectively. In [15] the images were obtained from diabetic subjects but there is no subject information in [12] [14]. Also, the resolution of our images is 2048×3072 which is greater than 1300×1000, 768×576 and 800×1000 as used in [12] [14] and [15], respectively. Our proposed system has high classification accuracy and low classification error rate for both *vein* and *artery* in our test image dataset. It should be pointed out that the resolution of our test images is higher than those used to test other classification algorithms reported in the literature and so our classification accuracy may differ with a different dataset. Also the classification result is highly dependent on segmentation results (for extracting centerline pixels). Moreover, choosing a different retinal zone, classifier and framework would likely impact on the classification performance. However, we conclude that our system performance is very promising. Further tests with much larger data sets are needed to declare suitability to support *a|v* classification in biomarker research. If successful in such tests, the algorithm will become a central component to the VAMPIRE software suite for automatic quantification of the retinal vasculature in fundus images.

Acknowledgment

This work is supported by Leverhulme Trust grant RPG-419 “Discovery of retinal biomarkers for genetics with large cross-linked datasets”.

References

[1] M. D. Abràmoff, M. K. Garvin, M.Sonka, “Retinal imaging and image analysis,” *IEEE reviews in biomedical engineering*, vol. 3, pp.169–208, 2010.

[2] N. Patton, T. M. Aslam, T. MacGillivray et al., “Retinal image analysis: concepts, applications and potential,” *Progress in Retinal and Eye Research*, vol. 25(1), pp. 99–127, 2006.

[3] W. E. Hart, M. Goldbaum, B. Côté, P. Kube, M. R. Nelson, “Measurement and classification of retinal vascular tortuosity,” *Intern. Journal of medical informatics*, vol. 53, pp. 239–52, 1999.

[4] T. Y. Wong, M. D. Knudtson, R. Klein, et al., “Computer-assisted measurement of retinal vessel diameters in the Beaver Dam Eye Study: methodology, correlation between eyes, and effect of refractive errors,” *American Academy of Ophthalmology*, pp. 1183–90, 2004

[5] Y. Jiang, A. B. Morris, “Blood vessel tracking in retinal images,” *Proc. of Image and Vision Computing*, Dec. 2007, pp. 126–131.

[6] H.Li, W. Hsu, M. Lee,T. Y. Wong, “Automatic grading of retinal vessel calibre,” *IEEE transactions on bio-medical engineering*,” vol. 52 (7), pp.1352-5, 2005.

[7] M. K. Ikram, J. C. M. Witteman et al., “ Retinal vessel diameters and risk of hypertension: the Rotterdam Study,” *Hypertension*: *Journal of the American Heart Association*, vol.47(2), pp.189–94, 2006.

[8] H. Leung et al., “Relationships between Age, Blood Pressure, and Retinal Vessel Diameters in an Older Population,” *Investigative Ophthalmology & Visual Science*, vol. 44(7), pp. 2900–2904, 2003.

[9] M. Niemeijer, B. van Ginneken, M. D. Abramoff, “Automatic classification of retinal vessels into arteries and veins,” *Proceedings of SPIE*, vol. 7260, 2009.

[10] C. Kondermann, D. Kondermann, M. Yan, “Blood vessel classification into arteries and veins in retinal images,” *Proceedings of SPIE*, vol. 6512, 2007.

[11] H. Narasimha-Iyer, J. M. Beach et al. “Automatic identification of retinal arteries and veins from dual-wavelength images using structural and functional features,” *IEEE transactions on bio-medical engineering*, vol. 54(8), pp. 1427–35, 2007.

[12] E. Grisan , A. Ruggeri., “A divide et impera strategy for automatic classification of retinal vessels into arteries and veins,” *Proc. of the 25th Annual International Conference of the IEEE Engineering in Medicine and Biology Society*, pp. 890– 893, 2003.

[13] M. Saez, S. González-Vázquez et al., "Development of an automated system to classify retinal vessels into arteries and veins,” *Computer methods and programs in biomedicine*, pp. 1–10, 2012.

[14] S. G. Vazquez, B. Cancela, N. Barreira et al., “On the Automatic Computation of the Arterio-Venous Ratio in Retinal Images: Using Minimal Paths for the Artery/Vein Classification,” *International Conference on Digital Image Computing: Techniques and Applications*, pp.599–604, 2010

[15] V. S. Joshi, M. K. Garvin, J. M. Reinhardt, M.D. Abramoff, “Automated artery-venous classification of retinal blood vessels based on structural mapping method,” *Proc.* of SPIE, vol. 8315, 2012.

[16] Y. Wu, X. Yang, K. Chan, “ Unsupervised color image segmentation based on Gaussian mixture model,” *4th Int. Conf. on Information, Communications and Signal Processing*, vol.1, pp. 15-18, 2003.

[17] R. Chrástek, M. Wolf, K. Donath, et al. “Automated segmentation of the optic nerve head for diagnosis of glaucoma. Medical image analysis,” 9(4), 297-314, 2005.

[18] J. Canny, “A computational approach to edge detection,” *IEEE Transaction on Pattern Analysis and Machine Intelligence*, vol. 8, pp. 679–698, 1986.

[19] A. Giachetti, K. S. Chin, E. Trucco et al. “Multiresolution localization and segmentation of the optical disc in fundus images using inpainted background and vessel information,” in *ICIP,* pp. 2145–2148, 2011.

[20] A. Perez-Rovira, T. MacGillivray et al., “Vampire: Vessel assessment and measurement platform for images of the retina,” in *Proc. IEEE Engineering in Medicine and Biology Society*, pp. 3391–3394, 2011.

[21] E. Trucco, L. Ballerini, D. Relan, et al., "Novel VAMPIRE algorithms for quantitative analysis of the retinal vasculature", *Proc. IEEE Intern. Conf. on Biosignal and Biosystems,* Rio de Janeiro, Brazil, Feb 2013.